Jakub BERNAT, Jakub KOŁOTA, Sławomir STĘPIEŃ

Poznan University of Technology, Chair of Computer Engineering

The FEM analysis of electromagnetic torque of hybrid stepper motor with different load

Streszczenie. *Artykuł prezentuje numeryczną metodę modelowania i symulacji hybrydowego silnika krokowego. Pole elektromagnetyczne modelu rozwiązano metodą elementów skończonych natomiast równania obwodowe zostały sprzężone z równaniami polowymi w jeden globalny układ równań niesymetrycznych. Ruch mechaniczny rotora silnika krokowego został zamodelowany używając równania różniczkowego drugiego stopnia, natomiast moment magnetyczny wyliczony został metodą Maxwella. Artykuł ukazuje w jaki sposób modyfikacja obciążenia rotora hybrydowego silnika krokowego wpływa na jego dynamikę i tętnienia momentu elektromagnetycznego. W pracy ukazano, iż analiza FEM takiego modelu może pozwalać, na optymalizację trybu obciążenia silnika krokowego w taki sposób, aby minimalizować niekorzystny wpływ tętnień momentu elektromagnetycznego. Wyniki prezentowanych symulacji zostały zweryfikowane laboratoryjnie i porównano je z wynikami otrzymanymi podczas pracy zestawu sprzętowego wykorzystującego nowoczesny sensor pomiaru momentu w silnikach typu FAST (ang. Force Angle Speed Torque).*

Abstract*. This paper presents the method of modeling and numerical simulation of a hybrid stepper motor. The problem is solved by the electromagnetic field modeling, using the time-stepping finite element method. Circuit equations are coupled with field equations creating one global system of non-symmetric equations. The mechanical motion of the rotor is determined by solving the second order differential motion equation. The magnetic torque is calculated by the Maxwell stress tensor. The paper shows how motor load modifications influence the response dynamic and torque ripples in the electromagnetic torque characteristic. It is shown that the FEM stepper model including the analysis of inertia controlled system can be used as support for improving tool and technics designed as predicting and controlling the electromagnetic torque ripples for motor drive applications. The simulations' results of electromagnetic torque are verified and compared with the results obtained from laboratory kit using FAST (ang. Force Angle Speed Torque) technology sensor.* ***Analiza FEM momentu elektromagnetycznego hybrydowego silnika krokowego z różnym obciążeniem****.*

Słowa kluczowe: hybrydowy silnik krokowy, metoda elementów skończonych, moment elektromagnetyczny
Keywords: hybrid stepper motor, Maxwell stress tensor, electromagnetic torque, finite element method (FEM)

Introduction

Along with dynamic development new industrial technology appears. Mechanics are looking for efficient, reliable, not demanding specialist service drives and control systems. Above-mentioned requirements should be performed in stepping motors systems, hence recently it is possible to notice significant growth of applications these solutions [6].

Stepper motors are electromagnetic incremental-motion devices which convert digital pulse inputs to the analog output motion. They can be successfully used in applications where a control of rotation angle, speed, position and synchronism is needed. Because of the inherent advantages listed previously, stepper motors have found their place in many different applications. Some of these include printers, plotters, office equipment, hard disk drivers, medical equipment, fax machines, automotive and many other [2,3,6].

In this paper a modeling method and a numerical simulation of the two-phased hybrid steppe motor is presented (Figure 1). The motor consists of slotted stator equipped with two bipolar coils and a rotor with no windings.

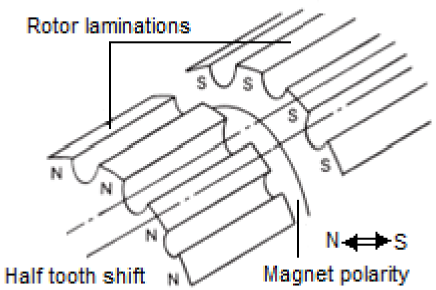

Fig. 1. A view of hybrid stepper motor rotor

Time stepping finite element approximation is applied to calculate the coupled field-circuit problem. High performance of motor drive applications require smooth torque with minimum torque ripples. The authors examined a few types of load which change dynamics of the motor, and the most interested of them are presented in this paper.

Obtained responses of examined models are compared with real hybrid stepper motor 57BYGH804 Wobit Company [9]. This is the universal motor, which can be controlled both bipolar and unipolar modes.

Table 1. The hybrid stepper motor parameters

Type of control	unipolar/bipolar
Nominal step	1.8 [angle]
Voltage supply	3.3 [V]
Current	3 [A]
Resistance	1,1 [Ω]
Inductance	1,4 [mH]
Torque	1,2 [Nm]
Inertia	440 [gcm^2]
Damping	0,0001 [Nms]
Weight	1,1 [kg]

Field-motion coupled model

Using the magnetic vector potential A and electric scalar potential V as electromagnetic field variables, the magnetic flux density B in conducting and non-conducting region ($\Omega_C \cup \Omega_N$) is defined as [10-13]:

$$\mathbf{B} = \nabla \times \mathbf{A} \ \text{ in } \Omega_C \cup \Omega_N \tag{1}$$

In this case, the boundary value problem in terms of potentials is expressed as follows:

$$\nabla \times \left(\frac{1}{\mu} \nabla \times \mathbf{A}(t) \right) = \mathbf{j}(t) + \mathbf{j}_m(t) \ \text{ in } \Omega_C \cup \Omega_N \tag{2}$$

$$\mathbf{j}_m(t) = \nabla \times M \tag{3}$$

where μ is a permeability, j(t) current density of the thin coil and M is magnetization vector. If voltage excitation is given, first the equations (1) expressed in term of magnetic vector potential must be considered as [1, 5]:

$$\begin{aligned} \frac{d}{dt} \oint_{l_1} \mathbf{A}(t) \mathbf{dl} + R_1 i_1(t) = u_1(t) \\ \frac{d}{dt} \oint_{l_2} \mathbf{A}(t) \mathbf{dl} + R_2 i_2(t) = u_2(t) \end{aligned} \tag{4}$$

where *R* is the winding resistance of a one phase, *i* is the phase current and *u* is the supply voltage. For two-phase voltage forced system above equations are expressed by matrix of dynamic impedances. Discrete form of (4) can be defined as bellow:

(5) $$\begin{bmatrix} Z_{11} & Z_{12} \\ Z_{21} & Z_{22} \end{bmatrix} \begin{bmatrix} i_1 \\ i_2 \end{bmatrix} = \begin{bmatrix} u_1 \\ u_2 \end{bmatrix}$$

where:

(6) $$Z_{ii} = R_i + \frac{1}{T_p I_i} \oint_{l_i} \mathbf{Adl}_i \; Z_{ik} = \frac{1}{T_p I_i} \oint_{l_k} \mathbf{Adl}_k$$

Global impedance matrix includes own impedances Z_{ii} and mutual impedance $Z_{jk} = Z_{kj}$. For $I_j = 1$ A (j=1,2) and for $I_{k \neq j} = 0$ (k=1,2) are performed calculations for matrix of impedance Z, next the current vector I in both coils are calculated from formulation:

(7) $$\mathbf{I} = \mathbf{Z}^{-1}\mathbf{U}$$

when a voltage vector U is known. Calculation of the force is performed using the Maxwell's stress tensor method. The force density is given by following formula:

(8) $$\mathbf{f} = \nabla \cdot \mathbf{T}$$

where T denotes modified Maxwell's stress tensor proposed as follows [2, 4]:

(9) $$\mathbf{T} = \begin{bmatrix} T_{11} & T_{12} & T_{13} \\ T_{21} & T_{22} & T_{23} \\ T_{31} & T_{32} & T_{33} \end{bmatrix}$$

where:

$$T_{11} = \frac{1}{2\mu_0} B_x^2 - \frac{1}{2}\mu_0 \left(H_y^2 + H_z^2\right), \; T_{12} = H_y B_x,$$

$$T_{13} = H_z B_x, \; T_{21} = H_x B_y, \; T_{23} = H_z B_y$$

$$T_{22} = \frac{1}{2\mu_0} B_y^2 - \frac{1}{2}\mu_0 \left(H_x^2 + H_z^2\right), \; T_{32} = H_y B_z$$

$$T_{33} = \frac{1}{2\mu_0} B_z^2 - \frac{1}{2}\mu_0 \left(H_x^2 + H_y^2\right), \; T_{31} = H_x B_z$$

The rotor displacement is evaluated by solution of the mechanical motion equation:

(10) $$J \frac{d^2\Theta}{dt^2} + b\frac{d\Theta}{dt} = T$$

where Θ is the rotor displacement, *J* is the rotor inertia, *b* is the damping coefficient, $T = T_E - T_L$ is the difference between the electromagnetic and the load torque.

The force is evaluated along a surface in the airgap around the rotor. The torque component *T* is obtained from the relationship [7]:

(11) $$\mathbf{T} = \oint_S \{\mathbf{r} \times \mathbf{P}\} \mathbf{dS}$$

where r is the position vector of the integration contour, P denotes the stress component defined around the rotor, dS is a surface segment. Only z-component of the torque $\mathbf{T} = [0 \quad 0 \quad T]^T$ is taken into consideration.

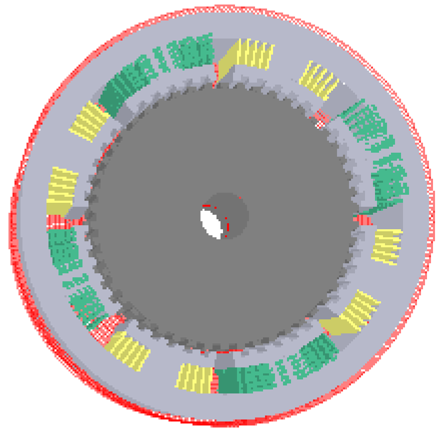

Fig. 2. Full 3D mesh of the hybrid stepper motor model

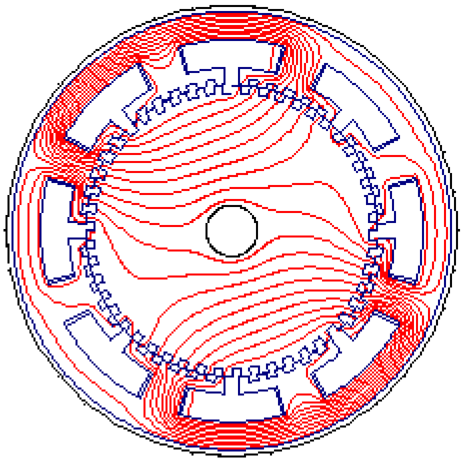

Fig. 3. Electromagnetic field distribution of the hybrid stepper motor

Results and discussion

The results obtained by FEM simulation model were verified in the real hardware environment shown in Figure 4. The measuring set was developed using the one of the newest methods of torque measurement technology FAST (ang. Force Angle Speed Torque). This technology is focused on the development and manufacture of non-contact sensors used to measure physical parameters such as torque. The sensor construction uses the inverse magnetostrictive effect also known as Villary effect. The Villary effect is the phenomenon of changing magnetization of a magnetic material when the material is stretched, compressed, twisted or bent.

The great advantage of the FAST technology is the ability to turn almost any steel shaft into a high precision sensor. This leads to very cost effective and robust sensor solution. Fast sensor used in the research (DFM22-2.5) can detect extremely high frequency load changes, can measure at very high RPM and is very compact.

The laboratory kit was coupled with MD100-M gauge, which is designed to work with non-contacting torque sensor. This gauge is widely applied, both in industry and research laboratories. It is easy to configure and operate, and the software is intuitive. MD100M is connected to a computer that is running MD100M-PC software. This connection allows to record and graphical visualization of measured values in real time [9]. The motor movement was inflicted by MI 1.8.8 programmer which is a hardware middleware between the workstation and the stepper motor controller. It uses WINMI control program, installed on the PC and communicates with the device via RS232 serial link.

It is especially useful wherever there is a need to perform complex, repetitive sequence of many parameters (both position and velocity) [9].

The control signals are realized by miniature controller SMC64v2 designed to work with two-phase stepper motor with bipolar (8 or 4 wires) or unipolar (6 wires) windings [9]. It allows full step control or broken step (2/4/5/8/10 or 16 parts) by forcing constant value of current in the motor regardless of the value of voltage supply.

In order to properly model a drive system both friction load and load inertia must be considered. Many simulations indicate that this is a crucial part of small drive system modeling. Gear drive system is one of the most popular way of connecting hybrid stepper motor.

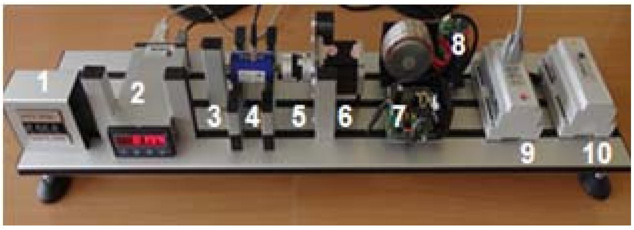

Fig. 4. The laboratory kit with FAST technology torque sensor *DFM22-2.5* :where: 1 – unipolar/bipolar control mode switch, 2 – torque gauge MD100M, 3 – gear drive system, 4 – DFM 22-2.5 torque sensor , 5 – clutch, 6 – stepper motor, 7 – motor controller, 8, 10 – voltage power supply, 9 – modul that defines the motor trajectory (PC connected)

When gears are used to drive a load, the inertia reflected to the motor is expressed by the following equation [9]:

$$J = \left(\frac{\alpha_1}{\alpha_2}\right)^2 * \left(J_2 + J_3\right) + J_1 \tag{12}$$

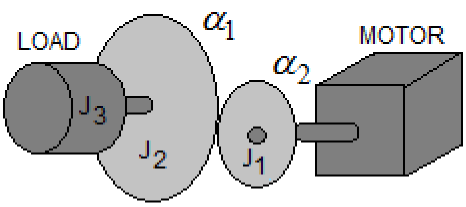

Fig. 5. Gear drive system model

where: J_1, J_2 and J_3 are inertias, α_1 is number of load gear teeth, α_2 is number of motor gear teeth. In the experiment shown in Figure 9 and Figure 10, the gears has been used with the following parameters: $J_1 = 1{,}12\,D^{-3} kg \cdot m^2$, $J_1 = 1{,}34\,D^{-3} kg \cdot m^2$, $J_3 = 0{,}29\,D^{-3} kg \cdot m^2$, $\alpha_2 = 44$ and $\alpha_1 = 18$.

The motor was controlled in bipolar full step mode with 3,3 [V] voltage excitation (Figure 6 and Table 2). During control without external load only half the bandwidth of the motor winding was used. In the second control mode (gear drive system) full bandwidth of the motor winding was supplied.

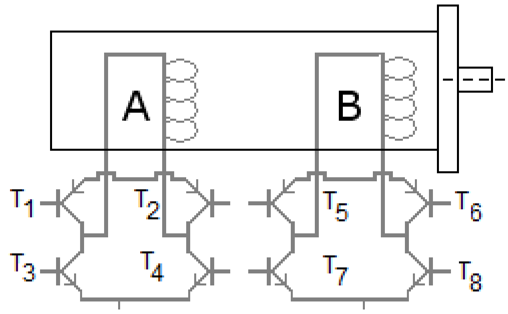

Fig. 6. Bipolar control mode of stepper motor

Table 2. Bipolar commutation of stepper motor

STEP	$T_{1,4}$	$T_{2,3}$	$T_{5,8}$	$T_{6,7}$
1	1	0	1	0
2	1	0	0	1
3	0	1	0	1
4	0	1	1	0
5	1	0	1	0

The analysis was focused on electromagnetic torque characteristics. The figures presented below compare data from a measurement of the stepper motor system equipped with a FAST torque sensor and FEM simulation of distributed parameters model.

First part of the research concerns one of the least favorable mode of stepping motor work - its revolutions without load. The torque characteristics (simulated and measured) are presented in Figure 7 and Figure 8. In this control mode appears unfavorable resonance frequency. The resonance is a result of no continue revolution's angular stator magnetic field. Consequently, deliver energy to rotor is pulsating and torque characteristic is oscillating.

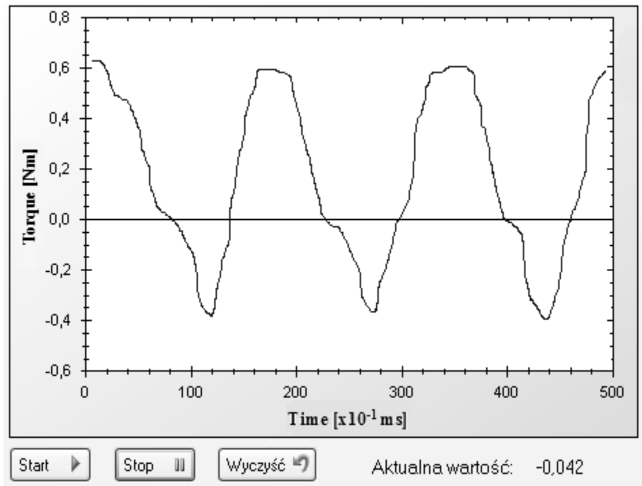

Fig. 7. Torque characteristic of stepper motor measured using FAST technique without external motor load

This can create problems of increased audible noise, fatigue of the shaft, and possible speed and displacement oscillations. The torque ripples could be significant reduced by appropriate designing the gear drive system.

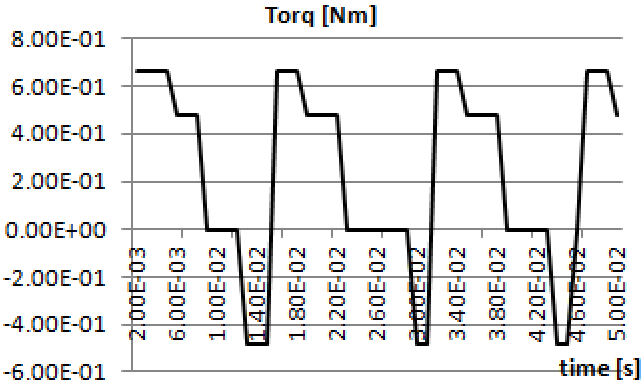

Fig. 8. Torque characteristic of stepper motor simulated using FEM method without external motor load

Including additional load inertia of controlled object reduces threshold of resonance frequency. In many cases, gear drive system is used as a method which enables to increase and stabilize torque dynamics [9]. Figure 9 and Figure 10 shows the results of electromagnetic torque obtained by considering additional model inertia shown in Equation 12. This research demonstrates the correctness of the implemented drive system. With accurate model of the motor with distributed parameters, the designer can adjust the optimal gear parameters to the control strategy.

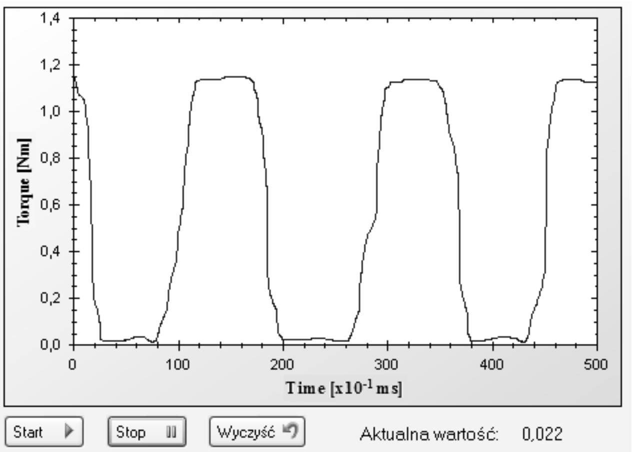

Fig. 9. Torque characteristic of stepper motor measured using FAST technique with external load

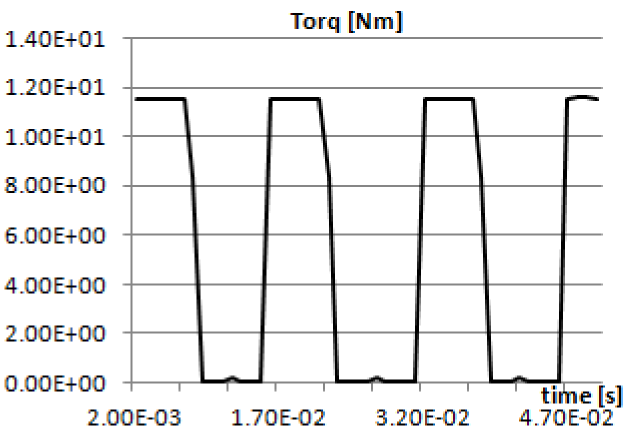

Fig. 10. Torque characteristic of stepper motor simulated using FEM method with external load

Conclusions

The main advantage in stepping motor control is good motion's dynamic, excellence response to acceleration, deceleration and step commands. Undoubtedly profitable with relation to other drive solutions is noncumulative positioning error (±5% of step angle)[1,5].

Unfortunately, a mechanical resonance phenomenon and torque ripples still constitute a big control problem. This can create problems of increased audible noise, fatigue of the shaft, and possible speed and displacement oscillations. Studying the change in torque at the model level allows to predict the course of electromagnetic torque. It is possible to adjust a rotor load and motor control more accurately on wide frequencies level.

The results show, that accurately coupled field–circuit model of hybrid stepper motor, calculating FEM usage, provides a useful tool to make detailed simulations. The suggested method and presented results can be used to design electromagnetic drives and may contribute to the improvement of the stepper motor drives dynamics

REFERENCES

[1] Bernat, J., Kołota, J., Stępień, S. (2009). Coupled field-motion model of variable reluctance stepper motor, *Przegląd Elektrotechniczny*, vol. 4, p. 210-213.
[2] Henrotte, F. (2004). *Handbook for the computation of electromagnetic forces in a continuos media,* ICS Newsletter, vol. 11, no. 2, p. 10-17.
[3] Rahman, K. M., Schulz S. E. (2002). *Design of high-efficiency and high torque density switched reluctance motor for vehicle propulsion*, IEEE Trans. Ind. Appl., vol. 38, p. 1500–1507.
[4] Stępień, S. (2010). *Determination of electromagnetic torque with on-line computation of the optimal radius of the integration contour*, Compel, vol. 29, p. 686-698.
[5] De Oliveira, A., Antunes, R., Kuo-Peng P., Sadowski, N., Dular, P. (2004). *Electrical machine analysis considering field – circuit – movement and skewing effects*, Compel, vol. 23, no. 4, p. 1080-1091.
[6] Vijayakumar, K., Karthikeyan , R., Paramasivam, S., Arumugam, R., Srinivas, K. (2008). *Switched Reluctance Motor Modeling, Design, Simulation, and Analysis: A Comprehensive Review*, IEEE Trans. Mag., vol. 44, p. 4605-4617.
[7] Stepien, S., Patecki, A. (2006). *Modeling and Position Control of Voltage Forced Electromechanical Actuator*, Compel, vol. 25, no. 2, p. 412-426.
[8] Panda, S.K., Xu, J.X., Qian, W. (2008). *Review of torque ripple minimization in PM synchronous motor drives, Power and Energy Society General* Meeting, Conversion and Delivery of Electrical Energy in the 21st century, p. 1-6.
[9] WObit Company (2012). Stepper motors. Retrieved on 4. 3. 2012, from http://www.silniki.pl.
[10] Biro, O., Preis, K. (1989). *On the Use of the Magnetic Vector Potential in the Finite Element Analysis of Three-Dimensional Eddy Current*, IEEE Trans. Mag., vol. 25, p. 3145-59.
[11] Hameyer, K., Bellmans, R. (1999). *Numerical modelling and design of electrical machines and devices*, Southampton, WIT Press.
[12] Lowther, D.A. (2003). *Automating the Design of Low Frequency Electromagnetic Devices - A Sensitive Issue*, Compel, vol. 22, p. 630-42.
[13] Sykulski, J., Stoll, J., Sikora, R., Pawluk, K., Turowski, J., Zakrzewski, K. (1995). *Computational magnetics*, Chapman & Hall, London.

Autorzy*: dr inż. Jakub Bernat, Poznan University of Technology, Chair of Computer Engineering, ul. Piotrowo 3a, 60-965 Poznan, E-mail:* Jakub.Bernat@put.poznan.pl;
dr inż. Jakub Kołota, Poznan University of Technology, Chair of Computer Engineering, ul. Piotrowo 3a, 60-965 Poznan, E-mail: Jakub.Kolota@put.poznan.pl;
dr inż. Sławomir Stępień, Poznan University of Technology, Chair of Computer Engineering, ul. Piotrowo 3a, 60-965 Poznan, E-mail: Slawomir.Stepien@put.poznan.pl.